

## Numerical Simulation of the Oxidant's Temperature and Influence on the Liquid Fuel Combustion Processes at High Pressures

A. Askarova, S. Bolegenova, Bolegenova Symbat, I. Berezovskaya, Sh. Ospanova,  
Zh. Shortanbayeva, A. Maksutkhanova, G. Mukasheva and A. Ergalieva  
Al-Farabi Kazakh National University, Almaty, Kazakhstan

---

**Abstract:** This study is devoted to the study of important from the view point of modern physics of numerical modeling of injection, ignition and combustion of liquid fuel at high pressures. It was investigated the oxidant's temperature and influence on the liquid fuel combustion processes at high pressures. In the course of work were obtained distribution of the gas temperature, concentration of combustion products, dispersion of particles for two types of fuels and distribution of velocity.

**Key words:** Numerical study, combustion chamber, high pressure, temperature, velocity

---

### INTRODUCTION

In our century of scientific and technical progress and advances in the field of computerization and globalization the science is developing every day. With the development of computer technology which has already become an intelligent assistant of man have achieved considerable success in addressing contemporary problems of thermal physics and the physics of combustion and explosion associated with the effective use of fuel resources and taking into account economic and environmental aspects of the process of different fuels burning.

Currently, one of the effective ways of theoretical investigation is a numerical experiment. It is based on the using of mathematical models of real processes. It is known that in the furnaces of power plants burned solid, liquid and gaseous fuel, so the using of a numerical experiment with attraction of means of computer technology to develop new technologies that require low cost and improved methods for the numerical implementation of systems of differential equations describing the processes of heat and mass transfer in the combustion chambers (Sabel'nikov *et al.*, 2011).

Numerical investigation of burning liquid fuels is a difficult task of thermal physics as it requires consideration of many interrelated processes and phenomenon. Therefore, the computational experiment is becoming an increasingly important element of the study of processes of burning and design of various devices using the combustion process. We can certainly say that its role will increase in the future. Therefore, all the more prevalent in thermal physics receive the methods of

computational hydrodynamics because makes it possible to optimize the experiment based on its virtual prototype (Askarova *et al.*, 2014a).

The combustion of liquid fuels has a number of specific features caused the chemical reaction in a dynamic and thermal interaction of reagents, intensive mass transfer in phase transformations as well as the dependence of the process parameters of the thermodynamic state of the system and its structural characteristics. As the study of combustion is not impossible without detailed study that comes to the problem of the fundamental study of consistent patterns of heat and mass transfer processes on different fuels burning. Numerical study of liquid fuels combustion is a challenge of the thermal physics as it requires a large number of related accounting processes and phenomena.

Therefore, the computational experiment is becoming an increasingly important element of the study of combustion processes and design of various devices that use the combustion process. It's safe to say that its role will increase in the future. Therefore, in the thermal physics methods of computational fluid dynamics is spreading increasingly, since it is possible to optimize the experiment based on its virtual prototype. Up to date it becomes increasingly clear that the problems arising in aero and hydrodynamics in the numerical solution of the Navier-Stokes equations are unlikely to be resolved.

Many scholars who specialize in the field of computational fluid dynamics and heat power engineering conducted similar researches in the modeling of the combustion of liquid and solid fuels (Askarova *et al.*, 2014b, c). In their research by researchers was used chemical model of pulverized coal combustion which

takes into account the integral component of the fuel oxidation reaction to the stable final products of the reaction (Askarova *et al.*, 2014d, 2012a, b, 2015; Messerle *et al.*, 2010). This model is the formation of the final products of oxidation is also used by us in the research.

Numerical experiments are investigated in the combustion chamber. It is a cylinder which the height equal to 15 cm, the diameter is 4 cm. After the injection, there is a rapid evaporation of fuel and the combustion is in the gas phase. The burning time of fuel is 4 msec. Time of injection of fuel droplets is 1.4 msec. The temperature of the walls of the combustion chamber is 353 K. The initial temperature of gas in the chamber is 900 K. The temperature of the liquid fuel is 300 K. The initial mean radius of injecting drops is 3 μm.

### MATH

Due to the increasing use of numerical studies in solving scientific and technical problems it is important to ensure the greatest possible scientific and practical «harvest». This is possible only with the deep penetration of mathematical modeling in a particular subject area. Solution of the spray and combustion of liquid fuels by means of numerical modeling using differential equations that describe the turbulent flow in the presence of chemical reactions and are presented by the basic equations: continuity, motion, internal energy, k-ε turbulence model as well as initial and boundary conditions.

Main equations of mathematical model of dispersion and combustion of spray of liquid fuel are presented below. Continuity equation for component m:

$$\frac{\partial \rho_m}{\partial t} + \bar{\nabla}(\rho_m \bar{u}) = \bar{\nabla} \left[ \rho D \bar{\nabla} \left( \frac{\rho_m}{\rho} \right) \right] + \dot{\rho}_m^c + \dot{\rho}_m^s \delta_{m1} \quad (1)$$

Where:

- $\rho_m$  = The mass density of species m
- $\rho$  = The total mass density
- $\bar{u}$  = The fluid velocity. We assume Fick's Law diffusion with a single diffusion coefficient D
- $\dot{\rho}_m^c$  and  $\dot{\rho}_m^s$  = Source terms due to chemistry and the spray, respectively. Species 1 is the species of which the spray droplets are composed
- $\delta$  = The dirac delta function

By summing Eq. 1 over all species we obtain the total fluid density equation where mass is conserved in chemical reactions:

$$\frac{\partial \rho}{\partial t} + \bar{\nabla}(\rho \bar{u}) = \dot{\rho}^s \quad (2)$$

The momentum equation for the fluid mixture is:

$$\frac{\partial(\rho \bar{u})}{\partial t} + \bar{\nabla}(\rho \bar{u} \bar{u}) = -\frac{1}{a^2} \bar{\nabla} p - A_0 \bar{\nabla} \left( \frac{2}{3} \rho k \right) + \bar{\nabla} \bar{\sigma} + \bar{F}^s + \rho \bar{g} \quad (3)$$

Where:

- $p$  = The fluid pressure
- $A_0$  = Zero in laminar calculations and unity when one of the turbulence models is used

The viscous stress tensor is Newtonian in form:

$$\sigma = \mu \left[ \bar{\nabla} \bar{u} + (\bar{\nabla} \bar{u})^T \right] + \lambda \bar{\nabla} \bar{u} \bar{I} \quad (4)$$

The superscript T denotes the transpose and  $\bar{I}$  is the unit dyadic.  $\bar{F}^s$  is the rate of momentum gain per unit volume due to the spray. The specific body force  $g$  is assumed constant. The internal energy equation is:

$$\frac{\partial(\rho I)}{\partial t} + \bar{\nabla}(\rho I \bar{u}) = -p \bar{\nabla} \bar{u} + (1-A_0) \sigma \bar{\nabla} \bar{u} - \bar{\nabla} \bar{J} + A_0 \rho \epsilon + \dot{Q}^c + \dot{Q}^s \quad (5)$$

where, I is the specific internal energy, exclusive of chemical energy. The heat flux vector  $\bar{J}$  is the sum of contributions due to heat conduction and enthalpy diffusion:

$$\bar{J} = K \bar{\nabla} T - \rho D \sum_m h_m \bar{\nabla} \left( \frac{\rho_m}{\rho} \right) \quad (6)$$

Where:

- $T$  = The fluid temperature
- $h_m$  = The specific enthalpy of species m

When one of the turbulence models is in use ( $A_0 = 1$ ), two additional transport equations are solved for the turbulent kinetic energy  $k$  and its dissipation rate  $\epsilon$ :

$$\frac{\partial \rho k}{\partial t} + \bar{\nabla}(\rho k \bar{u}) = -\frac{2}{3} \rho k \bar{\nabla} \bar{u} + \bar{\sigma} : \bar{\nabla} \bar{u} + \bar{\nabla} \left[ \left( \frac{\mu}{Pr_k} \right) \bar{\nabla} k \right] - \rho \epsilon + \dot{W}^s \quad (7)$$

$$\frac{\partial \rho \epsilon}{\partial t} + \bar{\nabla}(\rho \epsilon \bar{u}) = -\left( \frac{2}{3} c_{\epsilon 1} - c_{\epsilon 3} \right) \rho \epsilon \bar{\nabla} \bar{u} + \bar{\nabla} \left[ \left( \frac{\mu}{Pr_\epsilon} \right) \bar{\nabla} \epsilon \right] + \frac{\epsilon}{k} \left[ c_{\epsilon 1} \bar{\sigma} : \bar{\nabla} \bar{u} - c_{\epsilon 2} \rho \epsilon + c_s \dot{W}^s \right] \quad (8)$$

These equations are the standard k-ε Model. The quantities  $c_{\epsilon 1}$ ,  $c_{\epsilon 2}$ ,  $c_{\epsilon 3}$ ,  $Pr_k$  and  $Pr_\epsilon$  are constants whose values are determined from experiments and

some theoretical considerations. In the present calculations using the standard values of these constants:  $c_{e1} = 1.44$ ;  $c_{e2} = 1.92$ ;  $c_{e3} = -1.0$ ;  $Pr_k = 1.0$ ;  $Pr_c = 1.3$ . The state relations are assumed to be those of an ideal gas mixture. Therefore:

$$p = R_0 T \sum_m \left( \frac{\rho_m}{W_m} \right) \quad (9)$$

where the expression for the specific internal energy is:

$$I(T) = \sum_m \left( \frac{\rho_m}{\rho} \right) I_m(T) \quad (10)$$

The expression for the specific heat at constant pressure is:

$$c_p(T) = \sum_m \left( \frac{\rho_m}{\rho} \right) c_{pm}(T) \quad (11)$$

The expression for the enthalpy is:

$$h_m(T) = I_m(T) + \frac{R_0 T}{W_m} \quad (12)$$

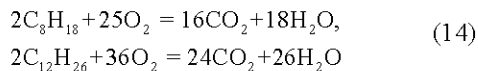
Where:

- $R_0$  = The universal gas constant
- $W_m$  = The molecular weight of species  $m$
- $I_m(T)$  = The specific internal energy of species  $m$
- $c_{pm}$  = The specific heat at constant pressure of species  $m$

The values of  $h_m(T)$  and  $c_{pm}(T)$  are taken from reference books. The conservation law component concentration is:

$$\frac{\partial}{\partial t}(\rho c_m) = -\frac{\partial}{\partial x_i}(\rho c_m u_i) + \frac{\partial}{\partial x_i} \left( \rho \cdot D_{c_m} \cdot \frac{\partial c_m}{\partial x_i} \right) + S_m \quad (13)$$

In this study, we carried out computational experiments to study the influence of the initial temperature on the concentration of vapors at high pressures. Octane and dodecane have been an object of research and their chemical formula has the following form as  $C_8H_{18}$  and  $C_{12}H_{26}$ . The chemical reaction are:



### RESULTS

This study was conducted numerical modeling of the liquid fuels combustion and the impact of gas temperature

in combustion chamber. Temperature in combustion chamber ranged from 700-1500 K. The values of the pressure in the chamber amounted to 100 bar for octane and 80 bar for dodecane as previously conducted research it was found that at these pressures the combustion process is the most effective, fuel injection velocity equal to  $350 \text{ m sec}^{-1}$  in both cases.

As a result of the computational experiment established that at pressure 80 bar and a temperature of 800 K and below the combustion does not occur as shown in Fig. 1, the dependence of the maximum temperature of the gas from the initial temperature of the combustion chamber.

The analysis of Fig. 2 shows, if oxidant in the combustion chamber has a temperature above 900 K in this case, there is a burning liquid fuel with great heat dissipation and heating of the camera. Thus, while combustion of octane at  $T = 900 \text{ K}$  stands out

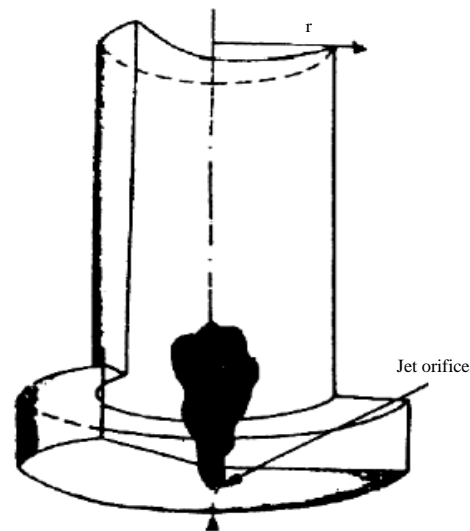


Fig. 1: The geometry of the combustion chamber

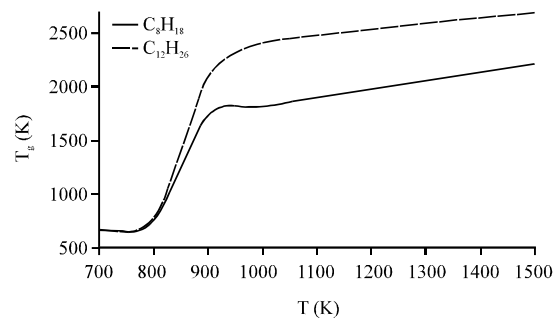


Fig. 2: Maximum gas temperature in combustion chamber depending on the initial temperature for octane  $C_8H_{18}$  and dodecane  $C_{12}H_{26}$

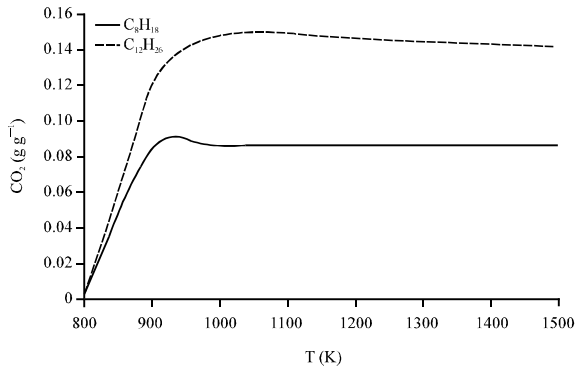


Fig. 3: Temperature dependence of the concentration of carbon dioxide for octane  $C_8H_{18}$  and dodecane  $C_{12}H_{26}$

$T_g = 1726$  K and as a result when  $T = 1500$  K allocated to  $T_g = 2208$  K. The greatest impact the initial temperature of the combustion chamber has on burning dodecane, since an increase in the initial temperature of 1500 K leads to the increase of the maximum temperature up to 2685 K.

Figure 3 demonstrates the maximum concentration of  $CO_2$  distribution for two burned fuels, depending on the initial gas temperature in combustion chamber. When burning dodecane concentration of produced carbon dioxide receives the greatest value  $0.148 \text{ g g}^{-1}$  at the initial temperature 1000 K and minimal  $0.120 \text{ g g}^{-1}$  at  $T = 900$  K. At combustion of octane at  $T = 900$  K and above, there was a slight increase in the concentration of  $CO_2$  which is equal to  $0.085 \text{ g g}^{-1}$ .

Figure 4 and 5 present some results of numerical experiments: distribution of drops of liquid fuel along the

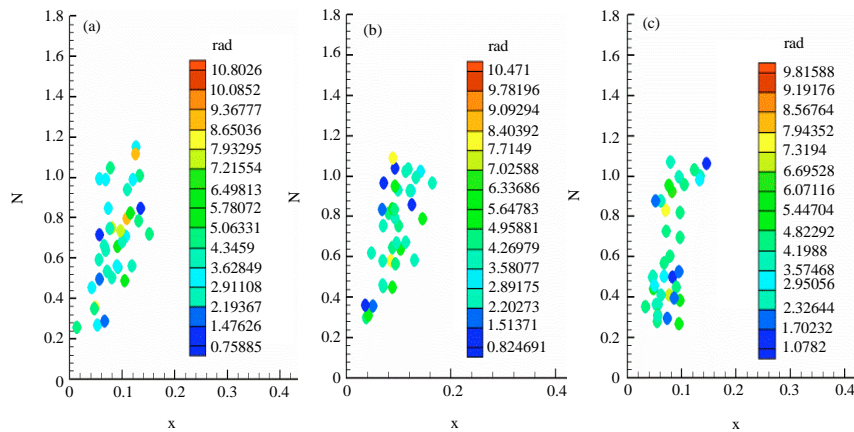


Fig. 4: Distribution of the octane's drops along the radius (rad, mm) in the space of the combustion chamber in a moment of time  $t = 0.8$  msec at different initial temperature: a) 700 K; b) 1000 K and c) 1500 K

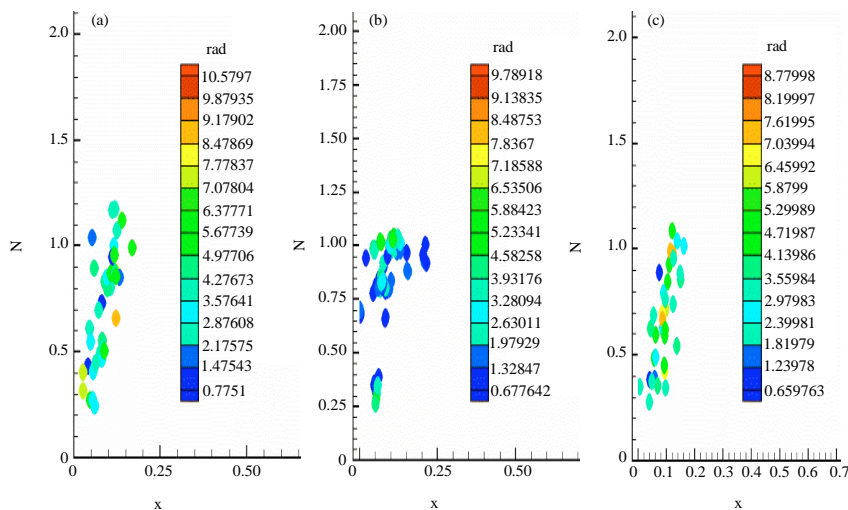


Fig. 5: Distribution of the dodecane's drops along the radius (rad, mm) in the space of the combustion chamber in a moment of time  $t = 0.8$  msec at different initial temperature: a) 700 K; b) 1000 K and c) 1500 K

radius (octane and dodecane), respectively. After analyzing the data, we can say that for obvious reasons with the increase of temperature in the combustion chamber of the liquid fuel drops size down a little.

Comparing the behaviour of octane and dodecane, we notice that the drop of both fuels are distributed in the same limits: rise to the same height of 1.2 cm at a given time and the width of the camera also there is a uniform

distribution of the drops to 0.2 cm, i.e., pair octane and dodecane reach the same height and their concentration on the axis coincides approximately.

There have also been obtained velocity distribution octane and dodecane in combustion chamber. Computing experiment was conducted at the initial rate of injection octane equal to  $350 \text{ m sec}^{-1}$ . The gas in the chamber was stationary. After the injection gas has gained some

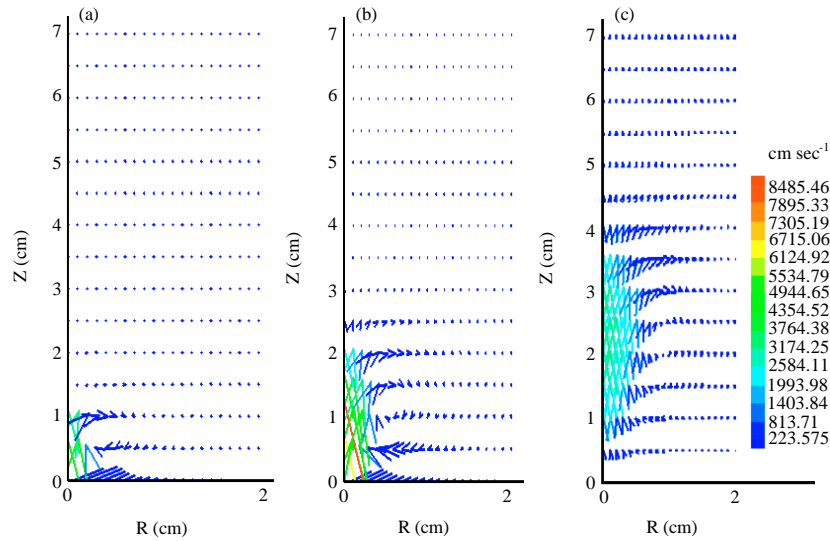


Fig. 6: The distribution of velocity in the combustion chamber at the combustion of octane: a)  $t_1 = 0.15 \text{ msec}$ ; b)  $t_2 = 0.6 \text{ msec}$  and c)  $t_3 = 1.8 \text{ msec}$

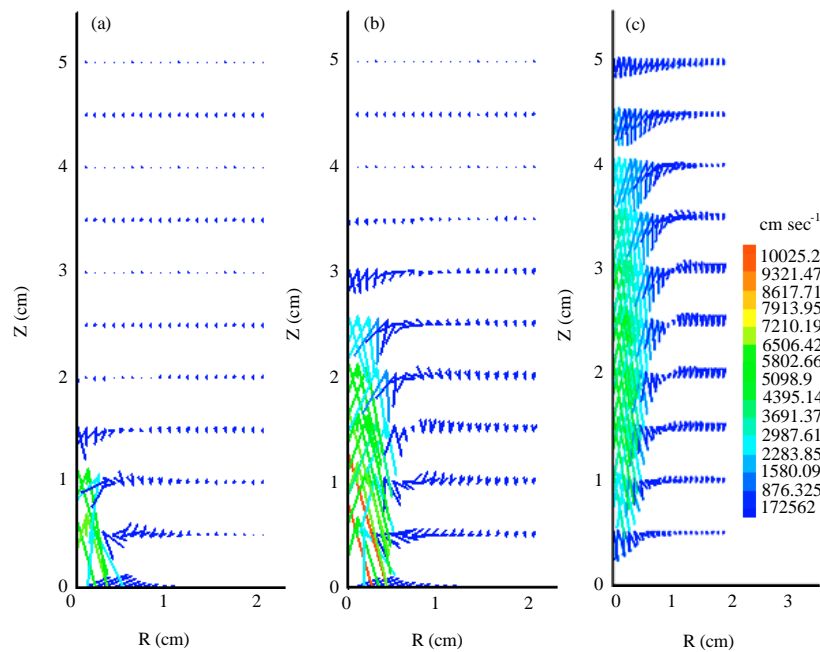


Fig. 7: The distribution of velocity in the combustion chamber at the combustion of dodecane: a)  $t_1 = 0.15 \text{ msec}$ ; b)  $t_2 = 0.6 \text{ msec}$  and c)  $t_3 = 1.8 \text{ msec}$

velocity. Analysis of Fig. 6 shows that the maximum gas velocity equal to  $8485 \text{ cm sec}^{-1}$  and is observed on the axis camera at a distance of 0.5 cm along its radius at the moment 0.6 msec. At the moment 1.8 msec gas velocity decreases and becomes equal to  $3600 \text{ cm sec}^{-1}$ , at the moment 0.15 msec is the minimum value  $2584 \text{ cm sec}^{-1}$ .

Drops of dodecane was injected with a velocity of  $350 \text{ m sec}^{-1}$  in the chamber where the gas was motionless. After that, the gas became engaged in liquid particles and its velocity has reached  $3691 \text{ cm sec}^{-1}$  when  $t_i = 0.15 \text{ msec}$ . Gas has acquired a maximum velocity for this type of fuel equal  $10025 \text{ cm sec}^{-1}$  and time 0.6 msec focused at a distance of 1 cm along the radius of the camera. To the moment of time equal to 1.8 msec, flow rate adopted value  $5802 \text{ cm sec}^{-1}$  (Fig. 7).

### CONCLUSION

There were have been conducted numerical investigation of the influence of the temperature in a cylindrical combustion chamber on the processes of ignition and of liquid fuels combustion of different species at high pressures in the specified initial conditions.

Distribution of the concentration of carbon dioxide showed that as expected, the more intense the reaction, the more  $\text{CO}_2$  is formed. At 900 K allocated to the minimum number of  $0.120 \text{ g g}^{-1}$  carbon dioxide for dodecane and for octane a low concentration of carbon dioxide equals  $0.085 \text{ g g}^{-1}$  which lies within the permissible limits.

Built distribution of drops for two kinds of liquid fuel (octane and dodecane) along the radius and temperature at the moment of time  $t = 0.8 \text{ msec}$  depending on the initial temperature of the gas in the chamber which has shown that couples octane and dodecane reach the same height and their concentration on the axis coincides approximately.

The most efficient combustion process dodecane and octane flows at the velocity of injection equal to  $350 \text{ m sec}^{-1}$ . Developed recommendations on determination of the optimal combustion in relation to the velocity at high pressures. At the velocity of injection  $350 \text{ m sec}^{-1}$  concentration of emission of harmful substances such as carbon dioxide is insignificant and lies within the permissible limits. Temperature in combustion chamber reaches maximum values. The results of computational experiments are confirmed by many scientific studies conducted in the field of research of processes of heat and mass transfer in reacting

high-temperature environments. The obtained results are of fundamental and practical importance and can be used for the development of the theory of gas and liquid fuels combustion.

### REFERENCES

- Askarova, A., S. Bolegenova, A. Bekmukhamet, S. Ospanova, Z. Gabitova, 2014a. Using 3D modeling technology for investigation of conventional combustion mode of BKZ-420-140-7C combustion chamber. *J. Eng. Appl. Sci.*, 9: 24-28.
- Askarova, A.S., A. Bekmukhamet, S.A. Bolegenova, M.T. Beketayeva and V. Maximov *et al.*, 2014b. Investigation of turbulence characteristics of burning process of the solid fuel in BKZ-420 combustion chamber. *WSEAS Trans. Heat Mass Transfer*, 9: 39-50.
- Askarova, A.S., A. Bekmukhamet, S.A. Bolegenova, M.T. Beketayeva and Y.V. Maximov *et al.*, 2014c. Numerical modeling of turbulence characteristics of burning process of the solid fuel in BKZ-420-140-7c combustion chamber. *Int. J. Mech.*, 8: 112-122.
- Askarova, A.S., V.E. Messerle, A.B. Ustimenko, S.A. Bolegenova and V.Y. Maksimov, 2014d. Numerical simulation of the coal combustion process initiated by a plasma source. *Thermophys. Aeromech.*, 21: 747-754.
- Askarova, A., S. Bolegenova, V. Maximov, M. Beketayeva and P. Safarik, 2015. Numerical modeling of pulverized coal combustion at thermal power plant boilers. *J. Therm. Sci.*, 24: 275-282.
- Askarova, A.S., S.A. Bolegenova, V.Y. Maximov and A. Bekmuhamet, 2012a. Mathematical simulation of pulverized coal in combustion chamber. *Procedia Eng.*, 42: 1150-1156.
- Askarova, A.S., S.A. Bolegenova, V.Y. Maximov, A. Bekmuhamet and Sh.S. Ospanova, 2012b. Numerical research of aerodynamic characteristics of combustion chamber BKZ-75 mining thermal power station. *J. Procedia Engin.*, 42: 1250-1259.
- Messerle, V.E., A.B. Ustimenko, A.S. Askarova and A.O. Nagibin, 2010. Pulverized coal torch combustion in a furnace with plasma-coal system. *Thermophys. Aeromech.*, 17: 435-444.
- Sabel'nikov, V., A. Chtab-Desportes and M. Gorokhovski, 2011. New sub-grid stochastic acceleration model in LES of high-reynolds-number flows. *Eur. Phys. J. B.*, 80: 177-187.